

Polarization rotation in parametric scattering of polaritons in semiconductor microcavities

A. Kavokin,¹ P. G. Lagoudakis,^{1,2} G. Malpuech^{1,2} and J. J. Baumberg²

¹LASMEA, UMR-6602, Université Blaise Pascal, 24 avenue des Landais, 63177, Aubiere, France

²Department of Physics and Astronomy, University of Southampton, Southampton, SO17 1BJ, United Kingdom

(Received 22 July 2002; revised manuscript received 15 November 2002; published 20 May 2003)

Polarization of light emitted by a semiconductor microcavity in the regime of a resonant parametric scattering of the exciton polaritons shows extremely strong and unusual dependence on the polarization of pumping light. This dependence is interpreted here using the pseudospin model and in the framework of a quasi-classical formalism where the parametric scattering is described as resonant four-wave mixing. We show that the optically induced splitting of the exciton-polariton eigenstate, both in linear and circular polarizations, is responsible for the observed polarization effects. The splitting in circular polarizations, achieving 0.5 meV, has been detected experimentally, while the splitting in linear polarizations, which is much weaker, only manifests itself in the pseudospin dynamics of the exciton polaritons.

DOI: 10.1103/PhysRevB.67.195321

PACS number(s): 78.45.+h, 71.36.+c, 42.65.-k, 78.67.-n

I. INTRODUCTION

Semiconductor microcavities have attracted a huge wave of interest since the discovery of stimulated scattering of exciton polaritons.¹ This effect revealed the bosonic nature of the exciton polaritons, the half-matter/half-light quasiparticles formed from strongly coupling an exciton resonance with an optical cavity mode. This has led to wide-ranging discussions about the possibility of Bose condensing the polaritons in microcavities that would open a way towards a new generation of optoelectronic devices (e.g., polariton lasers). The polariton spin dynamics during the course of this stimulated scattering has special importance for understanding the fundamental principles of the emission phenomenon. However, until now, very little has been known about the spin selection rules of the polariton scattering and previous experiments have shown a number of surprising effects that remain unexplained.

In this paper, we present a complete set of experimental data on the spin dynamics of resonantly excited exciton polaritons in a microcavity. This is quantitatively described within an original theoretical model. We demonstrate the existence of optically induced splittings of the exciton resonance in both linearly and in circularly polarized pumping of our system. We show that these splittings have a huge impact on the polarization dynamics of the polaritons.

We start by recalling the main features of the experiment in Ref. 1, which was the first observation of stimulated polariton scattering in semiconductor microcavities. A circularly polarized (σ^+) pump excited the cavity at the so-called “magic angle” and generated a coherent polariton population at the inflection point of the lower polariton branch. Then a circularly polarized probe pulse generated polaritons in the ground state that stimulated resonant scattering of polaritons created by the pump pulse to the probed state (at $k=0$). In the first instance, it seemed that the scattering of polaritons from the pumped state towards the ground state could only happen if the pump and the probe were cocircularly polarized (both σ^+ , for example). In case of cross-circularly polarized light, no stimulation should happen, at least if the spin-flip processes are not ultrafast as confirmed separately.²

It thus seemed possible to describe all the intermediate situations where both pump and probe are elliptically polarized by simply decomposing the pulse pump into σ^+ and σ^- components, one of which is strongly scattered and the other which is not scattered at all.

However, this picture has been completely ruled out by recent experimental results of Lagoudakis *et al.*³ who have reported extremely unusual polarization properties of a microcavity excited resonantly at the “magic angle” (Fig. 1). To briefly summarize these results, in the case of a linearly polarized pump pulse and circularly polarized probe pulse the observed signal was linearly polarized but with a plane of polarization rotated by 45° with respect to the pump polarization. In the case of elliptically polarized pump pulses, the signal also became elliptical while the direction of the main axis of the ellipse rotated as a function of the circularity of the pump. In the case of a purely circular pump, the polarization of the signal was also circular but its intensity was half that found for a linear pump. The polarization of the idler emission emerging at roughly twice the magic angle showed a similar behavior, although in the case of a linearly polarized pump the idler polarization was rotated by 90° with respect to the pump polarization. In the paper by La-

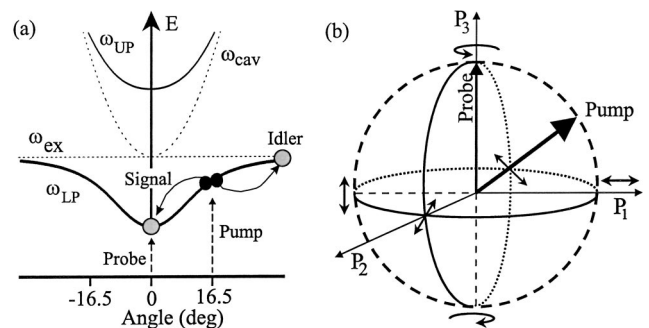


FIG. 1. (a) Dispersion relations of exciton (ω_{ex}), cavity photon (ω_{cav}), upper (ω_{UP}) and lower (ω_{LP}) polaritons, showing the dominant pair scattering for pump polaritons. (b) Poincaré sphere, representing polarizations: right/left circular at $P_3 = \pm 1$ and linear around the equator $P_3 = 0$. In experiments, the probe has always $P_3 = +1$, while the pump follows the dashed meridian.

goudakis *et al.*³ a qualitative interpretation of part of this data was presented in terms of the optical Josephson effect and stimulated spin-flip processes in the cavities. However, a detailed understanding of the observed effects has not been achieved.

This paper is organized as follows. In the next section a full set of experimental data on polarization and coherence of light emission by a resonantly excited microcavity in the parametric scattering regime will be presented. In Sec. III we present a semiclassical model that allows all the data to be fit using only two phenomenological parameters. In Sec. IV we derive these parameters using a pseudospin model. In the conclusion, remaining problems are discussed and possible extensions of the approach to describe polariton relaxation addressed.

In this section we give a short review of the experimental conditions, presented in detail in Ref. 3. In addition, we show new experimental data relevant to the spin dynamics of stimulated polariton scattering and reveal the behavior of the idler emission that proves to be vital for a rigorous explanation of the phenomena. The semiconductor microcavity used is a conventional $3\lambda_{ex}/2$, GaAs/In_{0.06}Ga_{0.94}/GaAs as described in Ref. 3. The experiment is performed at a temperature of 10 K in the pulsed regime. The incident beams are derived from a 100 fs mode-locked Ti:sapphire laser and are spectrally filtered inside zero-dispersion grating compressors in order to selectively excite the lower polariton (LP) branch. The resulting 3 ps pulses are set in the standard geometrical pump-probe configuration of resonant stimulated polariton scattering.¹ In particular, a pump pulse injects resonantly a reservoir of polaritons at the point of inflection of the LP branch and a weak probe pulse is sent at normal incidence onto the sample resonant to the LP branch, seeding polaritons of zero in-plane wave vector as shown in Fig. 1(a). The stimulated pair scattering process amplifies the probe over two orders of magnitude, resulting in a strong signal emission at normal incidence and gives rise to light emerging at a higher angle (called the idler) which comes from polaritons with energy and wave-vector set from energy and momentum conservation for the scattering event. Throughout the experiment the polarization of the probe pulse is kept right circular whereas we change the pump polarization from right to left circular hence varying linearly the relative spin populations of the pump-injected polaritons while keeping the pump intensity constant. This polarization selectivity in the pulsed domain allows the details of the Coulomb dipole-dipole scattering process to be sensitively investigated.

In order to keep track of the polarization of the different injected and emitted beams we analyze each polarization state using three Stokes parameters that correspond to the following polarization degrees:

$$P_1 = \frac{I_{\uparrow} - I_{\downarrow}}{I_{\uparrow} + I_{\downarrow}}, \quad P_2 = \frac{I_{\nearrow} - I_{\searrow}}{I_{\nearrow} + I_{\searrow}}, \quad P_3 = \frac{I_{\circ} - I_{\ominus}}{I_{\circ} + I_{\ominus}}, \quad (1)$$

where $I_{\uparrow, \downarrow, \nearrow, \searrow}$ are the intensities of linear components at $0^\circ, 90^\circ, \pm 45^\circ$ to the horizontal, and $I_{\circ, \ominus}$ are the circular components. In this way, we can express any polarization state as a vector in the orthogonal basis of Eq. (1) and we can

project it in the 3D polarization space, also known as Poincaré sphere, as Fig. 1(b) shows. Each of the Stokes parameters can be associated with a pseudospin S projection on three coordinate axes, so that $S_a = P_1$, $S_b = P_2$, $S_c = P_3$. This defines the pseudospin model that will be discussed in detail in Sec. IV.

Thus, throughout the experiment the polarization vector of the probe pulse is lying on the north pole of the Poincaré sphere. The polarization state of the pump pulse is moving along the meridian of the Poincaré sphere that passes through the equator at the states that corresponds to the horizontal and vertical linear polarizations, as shown in Fig. 1(b). We characterize the pumping light by its circular polarization degree

$$\rho = \frac{I^+ - I^-}{I^+ + I^-},$$

where I^+ is the intensity of the σ^+ component of pump pulse and I^- is the intensity of its σ^- component. The experimental values of the components that correspond to the three polarization degrees versus ρ for the emitted signal and idler are presented in Figs. 2(a)–2(c) and 3(a)–3(c) correspondingly. We observe that the linear components of both signal and idler exhibit oscillations versus circular polarization degree of pump, as was demonstrated for the signal emission in Ref. 3. However, from a direct comparison of Figs. 2(a)–2(c) and 3(a)–3(c) it becomes evident that the total intensities of signal and idler emission versus ρ exhibit very different behavior. To demonstrate clearly the difference we plot in Fig. 4(a) the total intensity of the emission versus pump circularity for both signal and idler. It is now evident that for the signal the total emitted light intensity is doubled for a linearly polarized pump compared to a σ^+ polarized pump, while in the case of idler emission the total intensity monotonically drops as the pump circular polarization degree decreases. Note also that the coherence degree of signal and idler emission is different, as seen in Figs. 4(b), 4(c). We define the coherence degree as the length of the polarization vector on Poincaré sphere. This parameter is always close to one for the signal while it is only about 0.5 for the idler at linear pumping. Enhancement of the idler coherence degree with polarization degree of the pump pulse is correlated with increasing overall intensity of idler emission, Fig. 4(a). These observations can be intuitively understood having in mind that the idler polaritons have longer life-times and can be efficiently elastically scattered with much higher probability than $k=0$ polaritons that have a huge photonic component. This shows that spin polarized excitons are more resistive and keep their polarization longer than linearly-polarized excitons. This should be true if spin-relaxation processes are slower than wave-vector relaxation, which is usually the case in quantum wells.

Furthermore, two new features appear from the comparison of signal and idler that will prove in the following sections to be of high importance for the understanding of the spin dynamics in the parametric scattering of polaritons. First, we observe that for *horizontal* linear pump polarization the signal emission is *diagonally* linear polarized. This fea-

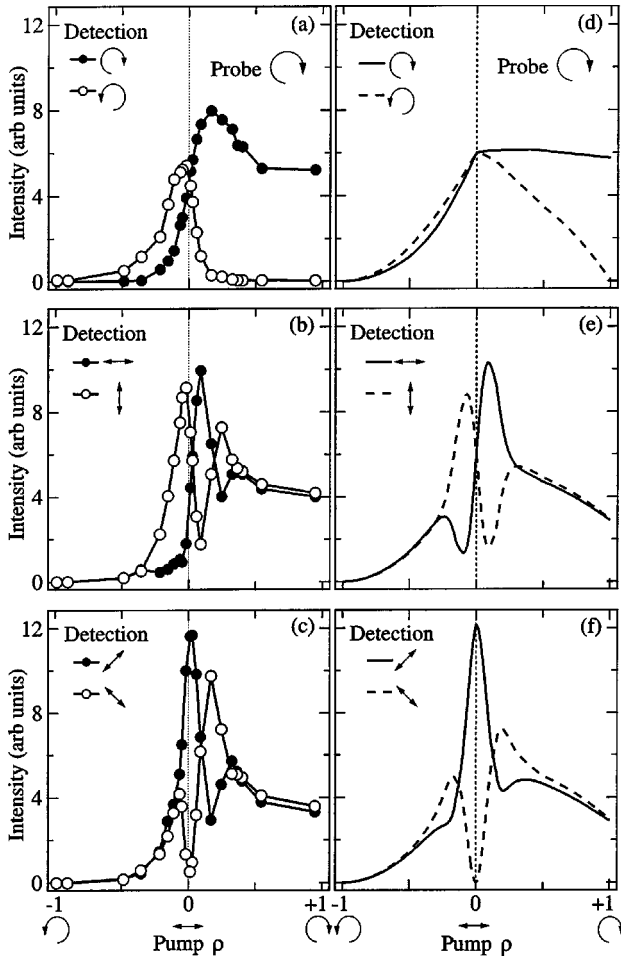


FIG. 2. Intensity of signal emission, decomposed into (a),(d) circular, (b),(e) linear, and (c),(f) linear diagonal polarizations, as a function of the pump circular polarization degree, where (a)–(c) show the experimental data and (d)–(f) show the theoretical predictions. The probe is σ^+ polarized.

ture cannot be derived from a stimulation effect of the polariton scattering, as in our case we seed only polaritons of one spin component (σ^+). As we will discuss in detail in Sec. III this effect originates from the pump-induced splitting of the exciton resonance in directions *both parallel and orthogonal* to the linear polarization, which rotates the polarization of signal polaritons.

Secondly, for the same (horizontally linear) pump polarization, the idler emission turns out to be *vertically* linear polarized. This feature is in fact in agreement with the calculation by Ciuti *et al.*⁴ which showed that the matrix element of exciton-exciton interactions V is dominated by the term coming from carrier-carrier exchange. This Coulomb interaction V is responsible for formation of signal and idler polariton populations.¹ Thus, the dipole moments of two polaritons that appear after the scattering should be oriented along the axis connecting two initial polaritons. In the case of linear pumping, the initial dipole moments of the interacting excitons are aligned along the X direction. Spin selection rules forbid the creation of circularly polarized excitons (which would not conserve angular momentum) thus polar-

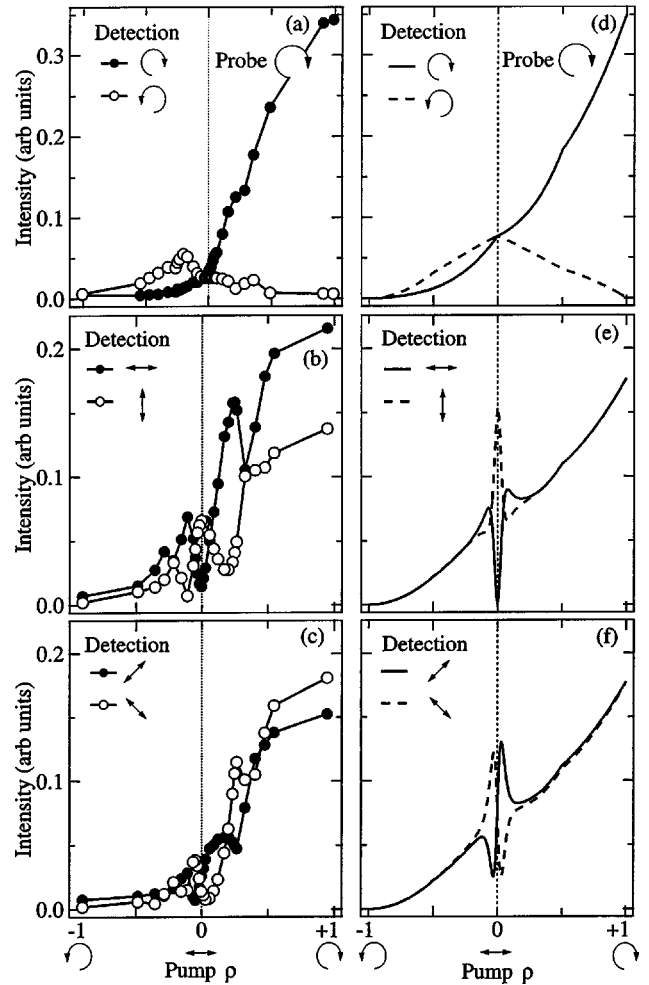


FIG. 3. Intensity of idler emission, decomposed into (a),(d) circular, (b),(e) linear, and (c),(f) linear diagonal polarizations, as a function of the pump circular polarization degree, where (a)–(c) show the experimental data and (d)–(f) show the theoretical predictions. The probe is σ^+ polarized.

iton dipoles can only scatter in the XY plane. Since the dipole-dipole interaction is strongly anisotropic, the polarization of the two resulting polaritons will be preferentially in the Y direction. This is indeed what the idler emission shows. The polarization of the signal cannot be described by using this argument because scattering to the signal state is stimulated by an injected probe pulse which constrains the pair scattering. In Table I we have summarized the polarization dependence of signal and idler for the basic pump polarizations (horizontal, cocircular, cross circular to the probe). The extremely pronounced and clear beats between the two linearly polarized components of emission both in signal and idler versus the circular polarization degree of the pump pulse will be interpreted in the next section.

II. SEMICLASSICAL MODEL

In this section, we will apply a semiclassical nonlinear optical formalism to describe the stimulated scattering of polaritons. First, we consider the modification to propagation

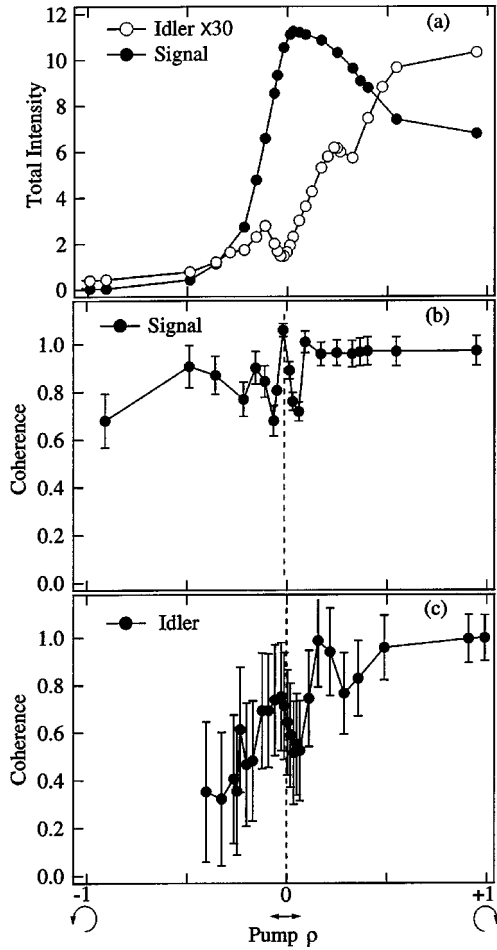


FIG. 4. (a) Total intensity of the emission of signal and idler as functions of the pump circular polarization degree. (b), (c) Coherence of signal and idler emission versus the pump circular polarization degree.

through the QW caused by optical pumping. Secondly, we consider diffraction of the pump pulse on the optical grating induced by the pump and probe pulses at the QW, which is nothing but a four-wave mixing process. The diffracted pulse

TABLE I. Polarization of emitted signal and idler in the pulsed and CW regime for the elementary pump polarizations.

Pulsed regime			
Pump	Probe	Signal	Idler
σ^+	σ^+	σ^+	σ^+
σ^-	σ^+	no signal	no idler
\leftrightarrow	σ^+	\nearrow	\downarrow
\updownarrow	σ^+	\searrow	\leftrightarrow
CW regime			
σ^+		σ^+	σ^+
σ^-		σ^-	σ^-
\leftrightarrow		nonpolarized	nonpolarized
\updownarrow		nonpolarized	nonpolarized

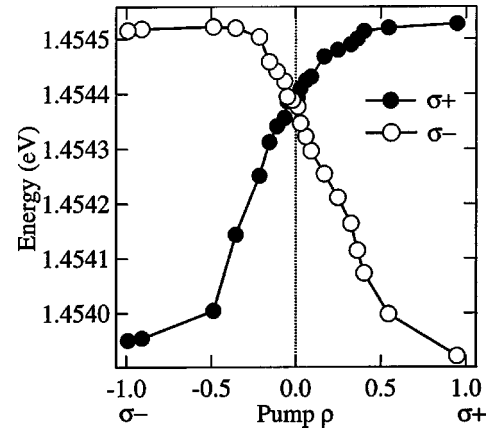


FIG. 5. Energies of σ^+ and σ^- exciton resonance as functions of the pump circular polarization degree.

then propagates freely within the cavity before tunneling out of the confining mirrors. The propagation of a diffracted light is described using the generalized scattering state technique.^{5,6}

The nonlinear aspect of the optical propagation in a strongly pumped cavity is accounted through the renormalization of the energies of the exciton resonance due to the exchange interaction of two spin-polarized excitonic populations resonantly excited by the pump pulse. This renormalization is not specific for the microcavities. It has been observed and theoretically described in quantum wells.^{7,8} The pump pulse generates large (σ^+ and σ^-) coherent polariton populations. In what follows, we assume that on the time scale of the experiment (several picoseconds) the polariton spin is conserved.² If the σ^+ population exceeds the σ^- one, it provokes a blueshift of the σ^+ exciton resonance and a redshift of the σ^- exciton resonance. The reason is the repulsive exchange interaction between two excitonic populations as has been observed by Martin *et al.*⁷ and theoretically described by Fernandez-Rossier *et al.*⁸ and Savasta *et al.*⁹ The main effect concerning our system is evidenced in Fig. 5, which shows the shift of the σ^+ and σ^- lower polariton peaks as a function of the pump circular polarization degree. This shift is responsible for a *giant Faraday rotation* of the polarization plane of light during its propagation within the cavity.^{10,11} This Faraday rotation coupled to the initial rotation produced by the self-diffraction of the probe (when the pump is linearly polarized) is mainly responsible of the experimental finding of Ref. 3. To gain an idea about the scale of the Faraday rotation effect in microcavities it is instructive to estimate analytically the amplitude of this rotation. In the following paragraph, we follow the method proposed in Ref. 10. We consider the transmission coefficient of the quantum well at the exciton resonance frequency which is given by

$$t_{\sigma^+, \sigma^-} = 1 + \frac{i\Gamma_0}{\omega_0^{\sigma^+, \sigma^-} - \omega - i(\gamma + \Gamma_0)}, \quad (2)$$

where $\omega_0^{\sigma^+, \sigma^-}$ is the exciton resonance frequency in the two polarizations, Γ_0 is the exciton radiative decay rate, and γ is the exciton nonradiative decay rate. If the inhomogeneous

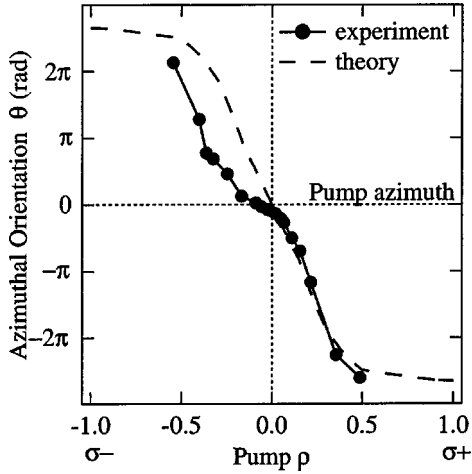


FIG. 6. Rotation angle of the linear polarization of signal emission as a function of the pump circular polarization degree.

broadening is neglected, the polarization plane of a linearly polarized light passing through the QW rotates by the angle

$$\varphi = \frac{(\omega_0^{\sigma^-} - \omega_0^{\sigma^+})\Gamma_0}{(\gamma + \Gamma_0)^2}. \quad (3)$$

In the case of a microcavity, the light emitted by a QW circulates many times between the mirrors thus accumulating an enhanced rotation before escaping the cavity. The amplitude of the emitted light can be found from

$$E = t_1 + t_1 r_1 e^{i\varphi} + t_1 r_1^2 e^{2i\varphi} + \dots = \frac{t_1}{1 - r_1 e^{i\varphi}}, \quad (4)$$

where r_1 and t_1 are the reflection and transmission coefficient of the Bragg mirror, respectively. The angle of resulting rotation of the linear polarization is

$$\theta_F = \arg(E) = \frac{r_1 \sin \varphi}{1 - r_1 \cos \varphi}. \quad (5)$$

Figure 6 shows the evolution of θ_F calculated using Eq. (5) vs the circular polarization degree of the pump pulse using the splitting $(\omega_0^{\sigma^-} - \omega_0^{\sigma^+})$ taken from the experimental data shown in Fig. 5. The points show the experimentally measured polarization rotation angle of the signal emission. One can clearly see that the rotation of the polarization plane by more than 2π observed experimentally is due to the Faraday rotation of the light polarization which is induced by the spin-split polariton resonance.

We now describe a procedure that allows us to calculate numerically all the polarization characteristics of the emitted light.¹² We will represent an electric field of any wave propagating in our structure as a vector

$$\vec{E} = \begin{bmatrix} E_X \\ E_Y \end{bmatrix}, \quad (6)$$

where E_X, E_Y are the field components in the plane of the microcavity. We consider the diffraction of the pump pulse

on a polarization grating created in the plane of the quantum well by pump and probe pulses near the exciton resonance frequency. The amplitude of light diffracted by a quantum well is a product

$$E_\alpha^{\text{sig}} = T_{\alpha\beta\gamma\delta} P_\beta P_\gamma^* S_\delta, \quad (7)$$

where $\alpha, \beta, \gamma, \delta$ take the values X or Y , P_β, P_γ are the components of the pump pulse, S_δ are the components of the probe pulse. We have omitted the diffraction of the pump pulse on the optical grating induced by the pump signal and pump idler pulses because at the early times of the stimulated scattering the signal and idler amplitude is negligible. At longer times, scattering of the pump pulse on the grating formed by pump-signal and pump-idler are becoming important, but the polarization of signal (idler) must remain the same as in the very beginning of the scattering process, otherwise bosonic amplification of the scattering would be lost. Here and further, we shall also neglect higher order contributions to the diffracted field. The tensor T is unknown *a priori* but it should satisfy certain symmetry requirements. In order to reveal them we introduce the two-component matrix

$$M_{\alpha\delta} = T_{\alpha\beta\gamma\delta} P_\beta P_\gamma^*. \quad (8)$$

Rotational symmetry of the system allows us to decompose the matrix M into three terms

$$M_{\alpha\beta} = A(P_X P_X^* + P_Y P_Y^*) \delta_{\alpha\beta} + B(P_\alpha P_\beta^* + P_\beta P_\alpha^*) + C(P_\alpha P_\beta^* - P_\beta P_\alpha^*), \quad (9)$$

where A, B, C are constants independent of the pump and probe amplitudes, $*$ denotes the complex conjugate of the fields, and $\delta_{\alpha\beta}$ is the Kronecker delta symbol. The first term in the right part of Eq. (9) describes the isotropic optical response of the system. The second term yields the in-plane anisotropy induced by a linearly polarized component of the pump pulse. The third term describes the gyrotropy induced by a circularly polarized component of the pump pulse. In a quantum picture the second term reflects the energy splitting of the exciton resonance in X - and Y -linear polarizations, while the third term reflects the σ^+, σ^- polarized exciton energy splitting. Note that the second term vanishes for a purely circularly polarized pump while the third term vanishes if the pump is purely linearly polarized.

As long as $A \neq 0$, its specific value does not change the dynamics observed, so we take for simplicity $A = 1$. Correct degrees of signal and idler polarizations at purely linear pumping can only be obtained using the following choice of B : $B = (i-1)A/2$ for the signal, $B = -A/2$ for the idler. In order to have a circularly polarized emission at purely circular pumping it is sufficient to keep C imaginary. In order to have a correct course of the emission intensity versus ρ we must choose $C = iA/8$ for the signal, $C = 2iA/3$ for the idler.

Note that at this stage the coefficients B and C are nothing but free parameters of a phenomenological model. In the next section we will justify their choice from a microscopic model using the pseudospin formalism. From the point of view of nonlinear optics Eqs. (7)–(9) fully describe the po-

larization of light diffracted at a quantum well. In order to account for the intensity dependence of the stimulation one should multiply the amplitude of Eq. (7) by a prefactor f that reflects the dependence of the observed scattering efficiency on the polarization of the pump pulse. This incorporates the spin selection rules found in Ref. 1 which are not yet included in the nonlinear mixing. In order to derive $f(\rho)$ we follow experiment in taking the efficiency of spontaneous scattering of exciton polaritons equal to zero. This is the case for a fully σ^- -polarized pump, whose stimulated scattering by a fully σ^+ -polarized probe is forbidden when spin-flip processes are excluded. Thus we impose the condition $f(-1)=0$, which arises from the experimental observations. Previous theories have shown that the energy shifts and the gain of the parametric amplification being considered depend on the repulsive potential of the exciton interaction and the coherently macroscopically occupied modes.¹³ This means that we expect that the efficiency of stimulated scattering should follow the same trend of ρ dependence as the energy shifts in Fig. 5. Thus we approximate this using a simple form of f :

$$f(\rho) = 1 + \rho \Theta(-\rho), \quad (10)$$

where $\Theta(x)$ is the Heavyside step function.

The saturation of the function f at $\rho > 0$ seems to be a consequence of the saturation of the pair scattering previously seen.² In principle f can be calculated microscopically taking into account the spin-configuration dependence of the exciton-exciton scattering probabilities, which would require heavy calculations beyond the scope of this work. Once emission of light by a quantum well is described by the amplitude of Eq. (7) multiplied by the function of Eq. (10), one can directly calculate polarization and intensity of light emitted by the cavity using the following procedure. The complex electric field of light is decomposed into two circularly polarized components

$$\begin{bmatrix} E_X^{\text{sig}} \\ E_Y^{\text{sig}} \end{bmatrix} = F^+ \begin{bmatrix} 1 \\ i \end{bmatrix} + F^- \begin{bmatrix} 1 \\ -i \end{bmatrix}, \quad (11)$$

where $F^{+(-)}$ are complex coefficients. Then we calculate separately propagation of σ^+ and σ^- components and find the amplitudes of both circularly polarized components of light emitted by the microcavity, using the generalized scattering state technique. Within this technique described in Refs. 5,6 we solve the complete Maxwell equations that describe the light propagation within the cavity. All multiple reflections of light within the structure are taken into account by a full transfer matrix procedure. As a result, the complex amplitudes of light emitted by the cavity $\tilde{F}^{+(-)}$ related to the two circular polarizations are obtained. Note that generally, if $\omega_0^- \neq \omega_0^+$, then $\tilde{F}^+/F^+ \neq \tilde{F}^-/F^-$ which results in a superimposed giant Faraday rotation effect.

This procedure for calculating the amplitude of light emitted by the cavity from the amplitude of light emitted by a quantum well is exact if no optical anisotropy of the cavity is present. That is, we assume that we can use the circular basis states for the photons inside the cavity, which is a reasonable

assumption given the negligible birefringence of the Bragg mirrors at these angles. In fact, a signature of such a breakdown would be the appearance of a nonzero circular polarization emitted for linear pumping.¹⁴ No experimental evidence of this was obtained [see Figs. 2(a)–2(c), 3(a)–3(c)].

The semiclassical model described here yields an impressive agreement with all the experimental data. Figures 2(d)–2(f) shows the calculated intensities of signal emission in two circular and four linear polarizations as a function of ρ . The agreement with the experimental measurements is substantial. Note especially that the period and amplitude of oscillations in linear polarizations, the ratio of intensities of the diagonal components of the emission at circular and linear pumping, and the polarization orientation at zero pumping, are all correctly predicted. Figures 3(d)–3(f) shows the same kind of theoretical calculations for the idler. The polarization is now found to rotate by 90° when the pump is linear. The oscillations remain, even if their visibility decreases. Another remarkable agreement is that the intensity of the idler is now higher when both pump and probe are circular, in contrast with what happens for the signal. In Fig. 7 we have plotted the calculated intensities of signal emission as in Figs. 2(d)–2(f) for different values of the parameter C . It is evident that parameter C has a negligible impact on the period and amplitude of oscillations in linear polarizations and on the polarization orientation at zero pumping. The only influence of parameter C that one could account for, is on the ratio of intensities of the different components of the emission at circular and linear pumping. Overall, the theory-experiment agreement is extremely good. The oscillations, overall intensity evolution versus the pump circularity and the 90° rotation of the linear pump are all correctly described.

III. PSEUDOSPIN MODEL

The advantages of the phenomenological model described in the previous section are twofold. It allows us to establish a connection between the observed oscillations in emitted linear polarization with the observed optically induced splitting of the exciton resonance in two circular polarizations via the well-known Faraday rotation effect. It also allows us to fit the model parameters B, C from the comparison of theory and experiment and thus to describe all the data with a very limited number of free parameters. The evident disadvantage of this model is that it does not explain in any way the choice of B and C . A micromodel analysis is needed to justify this choice.

In this section, we present a simple micromodel that confirms some of the assumptions made in the previous section. This micromodel involves a new effect, namely, the optically induced splitting of the exciton resonance in X - and Y -linear polarizations. The scale of this splitting is much less than the observed excitonic splitting in circular polarizations, discussed in the previous section. That is why this XY splitting has not been directly experimentally detected and does not manifest itself in the properties of linear propagation of light within the cavity. Our analysis shows nevertheless that this effect is present and moreover it has a huge influence on the

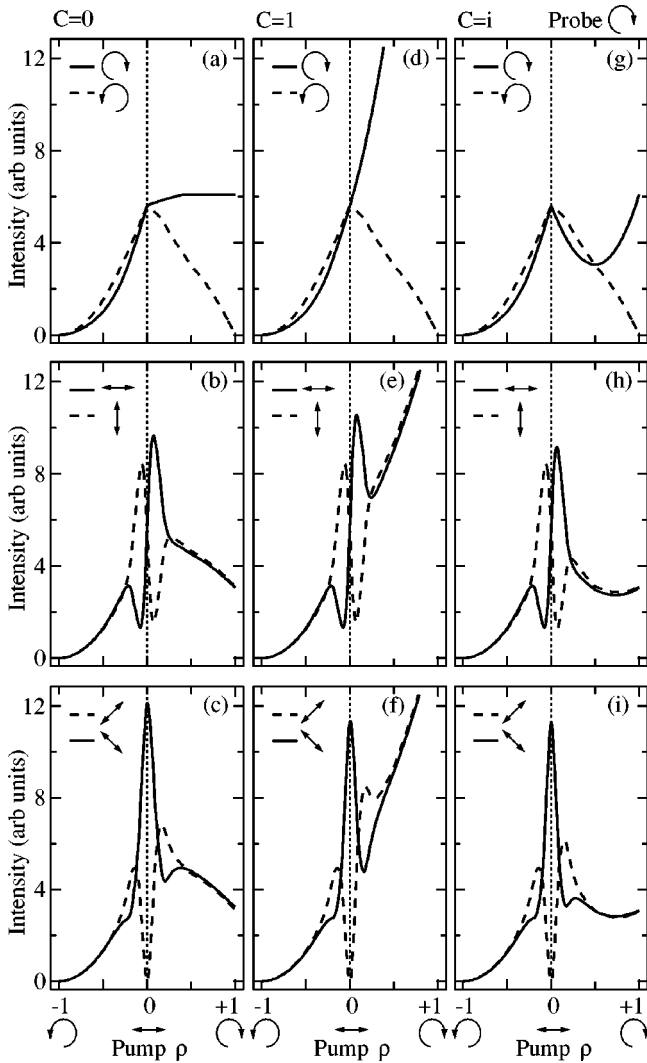


FIG. 7. Intensity of signal emission, decomposed into (a),(d),(g) circular, (b),(e),(h) linear, and (c),(f),(i) linear diagonal polarizations, as a function of the pump circular polarization degree, calculated for different values of parameter C [(a)–(c) for $C=0$, (d)–(f) for $C=1$, and (g)–(i) for $C=i$]. The probe is σ^+ polarized.

signal polarization for linear pumping.

In the following we will obtain an expression for the complex amplitude of light diffracted at a quantum well using the quantum theory of stimulated scattering.^{13,3} The stimulated scattering implies that the polaritons generated by the pump pulse scatter to the *same* quantum state as those from the probe pulse. However, in the case of linearly polarized pump and circularly polarized probe, this process is formally forbidden since it does not conserve the spin. On the other hand, due to the exchange interaction between polaritons from pump and probe, the polaritons excited by the probe pulse can start rotating their spins. This picture is illustrated in Fig. 8 showing precession of the pseudospin of the probe pulse around the pseudospin of the pump pulse. This process is described by the Hamiltonian¹⁴

$$\hat{H} = \frac{\hbar}{2}(\omega_i \sigma_i + \omega_z \sigma_z), \quad (12)$$

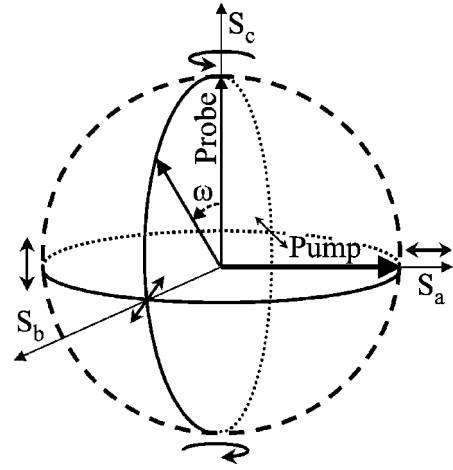


FIG. 8. Rotation of the pseudospin of the probe pulse around the effective magnetic field created by the much stronger pump pulse, shown schematically on the Poincaré sphere.

where σ_i are the Pauli matrices, $\hbar \omega_i$ is the pump-induced splitting of the exciton states linearly polarized along X and Y directions, $\hbar \omega_z$ is the pump-induced splitting of the circularly polarized exciton states σ^+ and σ^- . The pump pulse is much more intense than the probe pulse so that the reciprocal effect of pump pseudospin precession around the probe pseudospin can be neglected. The second term on the right hand side of Eq. (12) is zero in the case of linearly polarized pumping, while the first term can be nonzero. The optically induced splitting of the exciton resonance in two orthogonal linear polarizations has never been described theoretically nor observed experimentally to the best of our knowledge.¹⁵ However, it is not forbidden by symmetry and should exhibit the same features as the optically induced splitting of circular polarizations, namely, the exchange interaction between two exciton populations having different pseudospin projections. The exchange interaction of exciton populations with different dipole moment orientations but the same spin is apparently much less efficient than the exchange interaction involving spin flip. We estimate that the exciton resonance splitting in horizontal- and vertical-linear polarizations is of the order of few μeV . Nevertheless, it introduces precession of the pseudospin of the probe polaritons in the bc plane on the pseudospin Poincaré sphere (Fig. 8). This explains why the probe pseudospin starts to have a b component that corresponds to a diagonal linear in-plane polarization. Expressing the projections of the pseudospin of the probe pulse on the a and b axes using the Hamiltonian in Eq. (12), for positive ρ one can express the signal amplitude as

$$\begin{bmatrix} E_x^{\text{sig}} \\ E_y^{\text{sig}} \end{bmatrix} = \chi_a \begin{bmatrix} 1 \\ 0 \end{bmatrix} + \chi_b \begin{bmatrix} 1 \\ \pm 1 \end{bmatrix} + \chi_c \begin{bmatrix} 1 \\ i \end{bmatrix}, \quad (13)$$

where $\chi_{a,b,c}$ are the projections of the rotating pseudospin of the polaritons created by the probe pulse on a , b , and c axes given by

$$\chi_a = \xi \rho \sqrt{1 - \rho^2} (1 - \cos \omega \tau), \quad (14)$$

$$\chi_b = \xi \sqrt{1 - \rho^2} \sin \omega \tau, \quad (15)$$

$$\chi_c = \sqrt{\frac{\rho}{2}} \quad (16)$$

with $\omega = \sqrt{\omega_x^2 + \omega_z^2}$ and τ is the effective rotation time of the probe pulse. The normalization constant $\xi = \{(1 + \rho)[\rho^2(1 - \cos \omega \tau)^2 + 2 \sin^2 \omega \tau]\}^{-1/2}$, and the plus/minus sign on the right-hand side of Eq. (11) corresponds to the positive/negative value of the coefficient χ_b . Here we assumed that due to the spin conservation requirement, the percentage of the polaritons that contribute to the circularly polarized c component of the signal is ρ , while $(1 - \rho)$ polaritons contribute to the linearly polarized signal emission.

Comparing Eqs. (13) and (7)–(9), one can obtain the coefficients B , C for the signal. A remarkable fact is that the coefficient B is independent of the parameter $\omega \tau$ and is given by $B = (i - 1)/2$. This value can be easily understood from the pseudospin picture (Fig. 8) as the precession of the probe pseudospin about the effective pseudomagnetic field of the pump will always give rise to a diagonal component to the signal polarization which is then amplified. Thus, the pseudospin model yields exactly the same value of the coefficient B as the fit to the data. This is an important argument to justify that the basic assumption of the pseudospin model, namely the existence of a pump-induced $X - Y$ splitting of the exciton resonance is correct. To obtain the coefficient C [and additionally the function $f(\rho)$] one needs to know the polariton-polariton scattering rate dependence on ρ which is not described within this simple picture. In fact, this idea of the probe pseudospin precession only helps to describe the polarization of the signal emission. This latter is mostly dependent on coefficients A, B . The pseudospin precession does not have any apparent impact on the intensity of signal emission that is sensitive to C or f .

For the idler, Eq. (13) cannot apply since no initial polarized seed of the final scattering state is supplied, and thus there is more freedom in which spin of polaritons scattered into these states. The idler polaritons are initially all preferentially Y polarized (because of the directional anisotropy of the dipole-dipole interaction, as discussed in Sec. II). Subsequently, the light emitted in the idler direction experiences the Faraday rotation that leads to the oscillations in the idler polarization as a function of ρ .

To conclude this part, let us underline that the pseudospin model presented above is confirmed by the following additional experimental observations.

(i) Strongly enhanced signal emission is observed at delay times between the pump and probe pulses exceeding ~ 1 ps in the case of a linear pump and a circular probe.³ This confirms our assumption that the probe pulse should have a b component of pseudospin to stimulate the scattering. This b component is initially zero but appears with a ~ 1 ps delay as a result of the pseudospin precession.

(ii) The signal emission is nonpolarized in the CW regime for a linearly polarized pump. This experimental observation is in excellent agreement with the model prediction based on the fact that in this case there are no seeded probe pseu-

dospins and the spontaneous pair scattering over a long time yields equal populations of all possible emission polarizations.

IV. CONCLUSIONS

We have presented a semiclassical model that allows us to explain the surprising behavior of the polarized emission of resonantly excited microcavities. We show that the effect is governed by the diffraction of the pump pulse on the polarization grating created by the pump and probe pulses and by the resonant Faraday rotation of the polarization plane of light propagating in the cavity in the vicinity of the spin-split exciton resonance. The rotation of the polarization plane of the emitted light at 45° (for signal) and 90° (for idler) with respect to the polarization plane of a linearly polarized pump pulse is a consequence of the optically induced splitting of the exciton resonance for two *linear* polarizations (for signal) and of the anisotropy of the exciton-exciton exchange interaction (for idler). The oscillations of polarization of both signal and idler as a function of pump circularity is found to be a resonant Faraday rotation effect. We have presented a microscopic pseudospin model explaining the signal polarization behavior for the linear pump regime.

The theoretical analysis presented here was aimed at understanding the basic reasons for the surprising polarization effects observed experimentally. Briefly, these reasons can be summarized by optically induced excitonic splittings both in circular and linear polarizations, and the resulting giant Faraday effect. In order to reveal this essential physics we have used a very simple formalism that should be completed in further works, first of all, by a micromodel calculation of the polarization dependence of the exciton-exciton scattering rate. This would allow us to describe in detail the intensity of emission versus polarization degree of pumping which is only phenomenologically described by our present model. In future, we will extend the pseudospin model by developing kinetic equation for cavity polaritons in the three pseudospin projections. This would then become the appropriate tool to also analyze experimental polariton spin dynamics obtained under nonresonant pumping.⁷ Accurate theoretical description of the predicted effect of optically induced scattering of the exciton resonance in two linear polarizations deserves a separate work indeed. We underline that polariton spin dynamics in microcavities is an area extremely rich on new effects and not yet substantially investigated. We believe that this work will help understanding of a part of these effects.

ACKNOWLEDGMENTS

We have greatly benefited from the discussions with M.I. Dyakonov, who, in particular, has proposed to us to represent the matrix $M_{\alpha\beta}$ in the form of Eq. (8). We acknowledge very helpful discussions with K. Kavokin. This work has been supported by the EU RTN ‘‘CLERMONT’’ program, contract Nos. HPRN-CT-1999-00132, HPMT-CT-1999-00191, EPSRC GR/M43890, and HEFCE JR98SOBA.

- ¹P.G. Savvidis, J.J. Baumberg, R.M. Stevenson, M.S. Skolnick, D.M. Whittaker, and J.S. Roberts, Phys. Rev. Lett. **84**, 1547 (2000).
- ²P.G. Savvidis, J.J. Baumberg, R.M. Stevenson, M.S. Skolnick, D.M. Whittaker, and J.S. Roberts, Phys. Rev. B **62**, R13 278 (2000).
- ³P.G. Lagoudakis, P.G. Savvidis, J.J. Baumberg, D.M. Whittaker, P.R. Eastham, M.S. Skolnick, and J.S. Roberts, Phys. Rev. B **65**, 161310 (2002).
- ⁴C. Ciuti, V. Savona, C. Piermarocchi, A. Quattropani, and P. Schwendimann, Phys. Rev. B **58**, 7926 (1998).
- ⁵Guillaume Malpuech, Alexey Kavokin, Wolfgang Langbein, and Jørn M. Hvam, Phys. Rev. Lett. **85**, 650 (2000).
- ⁶Guillaume Malpuech and Alexey Kavokin, Semicond. Sci. Technol. **16**, R1 (2001).
- ⁷M.D. Martin, G. Aichmayr, L. Viña, and R. André, Phys. Status Solidi A **190**, 351 (2002).
- ⁸J. Fernández-Rossier and C. Tejedor, Phys. Rev. Lett. **78**, 4809 (1997).
- ⁹Salvatore Savasta, Omar Di Stefano, and Raffaello Girlanda, Phys. Rev. B **64**, 073306 (2001).
- ¹⁰A. Kavokin, M.R. Vladimirova, M.A. Kaliteevski, O. Lyngnes, J.D. Berger, H.M. Gibbs, and G. Khitrova, Phys. Rev. B **56**, 1087 (1997).
- ¹¹C. Flytzanis (private communication).
- ¹²Y.R. Shen, *Principles of Nonlinear Optics* (New York, Wiley, 1984), Chap. 10.
- ¹³P.G. Savvidis, C. Ciuti, J.J. Baumberg, D.M. Whittaker, M.S. Skolnick, and J.S. Roberts, Phys. Rev. B **64**, 075311 (2000).
- ¹⁴R.I. Dzhioev, H.M. Gibbs, E.L. Ivchenko, G. Khitrova, V.L. Korenev, M.N. Tkachuk, and B.P. Zakharchenya, Phys. Rev. B **56**, 13 405 (1997).
- ¹⁵J.L. Oudar, A. Migus, D. Hulin, G. Grillon, J. Etchepare, and A. Antonetti, Phys. Rev. Lett. **53**, 384 (1984).